

Tuning the band gap by using different capping agents in Mn²⁺ doped ZnS nanocrystals

PRINSA VERMA*, A. C.PANDEY^a, R. N. BHARGAVA^b

Allahabad University, Allahabad, India

^aIndian Space Research Organisation

^bNanocrystal Technolog, NewYork (USA)

We reported the wet chemical synthesis of the ZnS: Mn nanoparticles capped with different capping agents. The growth in particle size was arrested using inorganic and organic capping without significant change in photoluminescence intensity and variation in band gap with or without shell and activator were calculated. The particle size was determined using TEM/SAXS and peak broadening of XRD was found between 10-20 nm.

(Received March 19, 2009; accepted April 23, 2009)

Keywords: Nanocrystal, Band gap, Activators, ZnS

1. Introduction

In recent years doped semiconducting nanocrystals attracted great interest after the observation of enhanced luminescence efficiency and shortening of radiative lifetime by orders of magnitude from millisecond to nanoseconds[1]. These promising properties along with the possibility of synthesizing materials by bottom-up approach will bear a great potential for their application in a number of high technology areas such as high density displays, DNA markers, biosensors, light emitting diodes, lasers, etc [2,3] as these materials behave differently from bulk semiconductor material. With decreasing particle size, the band structure of the semiconductors changes, the band gap increases, and the edges of the bands splits into discrete energy levels. These so called quantum confinement effects have stimulated great interest in both basic and applied research [4,5]. In 1994, Bhargava and Gallagher [6] reported that doped nanocrystals of semiconductors can yield both high luminescence efficiencies and lifetime shortening from ms to ns at the same time. Intrinsic optical properties of ZnS nanostructures have been intensively studied to implement it on photonic devices.

It is difficult to achieve size selective synthesis confined in nano regime, by using the traditional approach [7, 8]. Chemical methods of synthesis have a further advantage of tunable surface properties of which can be affected by the adsorbed ions (for electrostatic stabilization) or the passivating polymer (Steric hindrance).

In this paper, we have discussed chemical synthesis of capped ZnS doped with manganese. Wet chemical routes are highly attractive to grow nanosystems because of their cost effectiveness, large area coverage and easy tunability of chemical conditions to control the growth pattern and crystal properties. Synthesis of doped ZnS is based on a precipitation reaction, in an organic solution of precursors,

whereas other methods are also being employed such as electro-deposition vapour transport process, polymer assisted grown, wet oxidation process, vapour solid (VS) process, vapour liquid solid (VLS) epitaxial synthesis, chemical vapour deposition (CVD) [9-14] and also having special environment such as high temperature, catalyst & some times inert gas flow. While, we report a simple surfactant and catalysts free wet chemical method for the nucleation and growth of ZnS nanopowder at room temperature. In the case of doped nanosystems, the crystal growth conditions as well as doping chemistry are to be simultaneously optimized to achieve substitutional placement of impurity ions at the host lattice to evoke required properties of interest, such as ferromagnetism, n or p type conductivity, luminescence, etc. Stabilization mechanism of nanoparticles can be categorized as-1) *Electrostatic Stabilization*- Involving the creation of a double layer of adsorbed ions over the nanoparticles resulting in columbic repulsion between approaching nanoparticles. 2) *Steric Hindrance*- Achieved by adsorption of polymer molecule over the nanoparticles. Osmotic repulsion felt between the polymer molecules due to localized increase in their concentration when polymer coated nanoparticles approach each other, keeps them (along with the nanoparticles) well separated.

Here manganese is used as dopant in our experiment. In a typical synthesis, zinc acetate and manganese acetate of varying molar ratios are mixed in ethanol along with 1% solution of polyvinyl alcohol/Silica Oxide (PVA/SiO₂). In the precipitation of multi- component materials, special attention is given to controlled co-precipitation condition in order to achieve chemical homogeneity of the final product. This is due to the fact that different ions often precipitate under different conditions of pH and temperature having different product constants. Hence a coarse control of the doping concentration can be achieved by tuning the reaction conditions [18, 19]. These nanoparticles are sterically stabilized by the capping agents

present in the reaction medium. Synthesis usually involves dissolution of zinc acetate in alcohol.

2. Experimental

Samples reported in this paper were prepared by co-precipitation reaction. In the typical precipitation of doped ZnS nanocrystals, 50 ml of 0.01M Mn(II)acetate solution is added to Zinc precursor (0.1M) in order to obtain required Mn concentration in the precipitating medium. Followed by this, the capping agent polyvinyl alcohol/Silica oxide (1% PVA/SiO₂) was added to the Zn²⁺ dopant precursor solution & allowed to mix very well for few minutes. Doped particles with PVA/SiO₂ capping were precipitated by slowly adding 50ml of 0.1M Na₂S solution to the above mixture. The precipitates were collected by centrifuging and washing several times with ethanol. Synthesis of ZnS: Mn²⁺ samples were also repeated after optimization of parameters at room temperature and low temperature (4°C) following the same procedure for the optimized parameters.

The nanoparticles synthesized thus were characterized by Transmission Electron Microscopy (TEM), X-ray Diffraction (XRD), Small Angle X-ray Scattering (SAXS) and Photo-Luminescence Spectroscopy. Crystallinity of the samples was studied using an X-ray diffractometer fitted with a Cu-K_{alpha} source.

3. Result and discussion

Fig 1 shows XRD pattern of the samples ZnS: Mn²⁺ capped with PVA and Silica oxide. Both the samples of ZnS: Mn shows that the nanoparticles exhibit the typical Wurtzite structure. The corresponding XRD peaks for ZnS (111), (200) and (311) corresponding to Wurtzite structure and confirmed with JCPDS card no. 36-1450. From the XRD line width, the mean crystalline domain sizes of Silica oxide and PVA capped Mn doped ZnS nanocrystals have been estimated to be around ~ 10 nm and ~ 20 nm respectively, using the Debye-Scherrer formula [25].

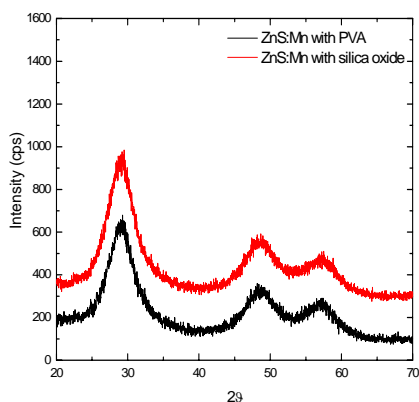


Fig .1 XRD Pattern of ZnS:Mn with silica oxide and PVA .

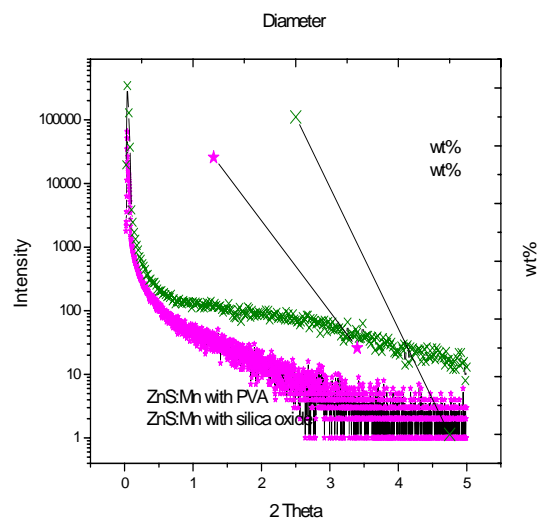


Fig.2 Small angle X-ray scattering pattern for ZnS coated with silica oxide and PVA.

By small angle X-ray scattering,(as in fig 2) the particles were of 10nm with a distribution of 70-80% capped with silica oxide while the particles were of 20nm with a distribution of 50-60% capped with PVA .Better particle size distribution achieved by silica oxide capping. Fig 3 shows PLE spectra, indicating ZnS:Mn capped with silica oxide peak at 268 nm while 330 nm with PVA capping. On illumination with a low power UV lamp a bright orange red glow is observed due to presence of Mn²⁺ trap centers slightly below the Fermi level of the band gap of ZnS [16,17]. This confirms that Manganese ions have been incorporated into the crystal structure of ZnS and is not present as amorphous MnS mixed with ZnS.

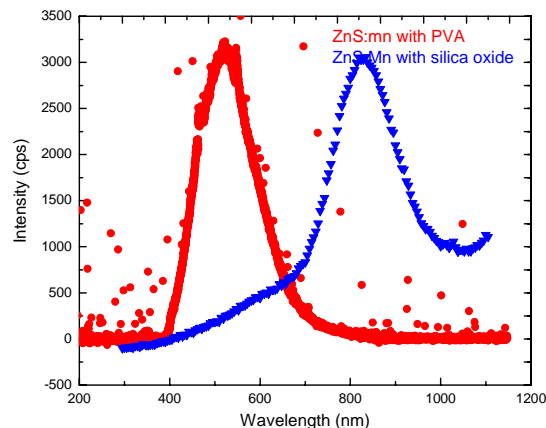


Fig 3. PLE Spectra of ZnS:Mn capped with PVA and silica oxide

The orange photoluminescence originates from a transition between the ⁴T₁ excited state and the ⁶A₁ ground state of the Mn²⁺ ion within a nano-crystalline ZnS lattice [20]. When an electron is prompted to the excited state, there are two main paths for electron to relax to the ground state. One is the relaxation process through surface defects, such as donors and acceptors. This relaxation will usually give rise to a non-radiative recombination and/or light emission at other wavelengths. The other emission is due to an intra-configurational 3d⁵ transition on the Mn²⁺ ion located within the bandgap of ZnS nanocrystals. This ⁴T₁ - ⁶A₁ energy transition gives rise to an orange photoluminescence [21].

Due to the heavy dependence of optical properties the size, (such as emission λ), the practical applications require that the size of the quantum dot be controlled precisely. Hence the present research activities associated with these quantum dots, are concentrating on the preparation of mono-dispersed size nanocrystals.

In general, quantum confinement shifts the energy levels of the conduction and valence bands apart, giving rise to a blue shift in the transition energy as the particle size decreases. Such phenomenon is also revealed in the absorption spectra, although the faint excitonic absorption peaks due to moderate size distribution of ZnS NPs. The relationship between the bandgap and size of NPs can be obtained using a number of models [22,23]. Using the effective mass model for spherical particles with the coulomb interaction term [22], the band gap E_g^* [eV] can be approximately written as

$$E_g^* \cong E_g^{\text{bulk}} + \frac{h^2 \pi^2}{2er^2} \left(\frac{1}{m_e} + \frac{1}{m_h} \right) - 1.8e^2 / 4\pi\epsilon\epsilon_0 r$$

Where E_g^{bulk} is the bulk energy gap, r is the particle radius, m_e is the effective mass of the electrons, m_h is the effective mass of the holes, ϵ is the relative permittivity, ϵ_0 is the permittivity of free space, h is Planck constant divided by 2π , and e is the charge of the electron. The polarization term included in this model is usually negligible.

By using all values we calculated band gap of ZnS capped with Silica oxide and PVA ~ 3.7 and ~ 4.0 eV respectively.

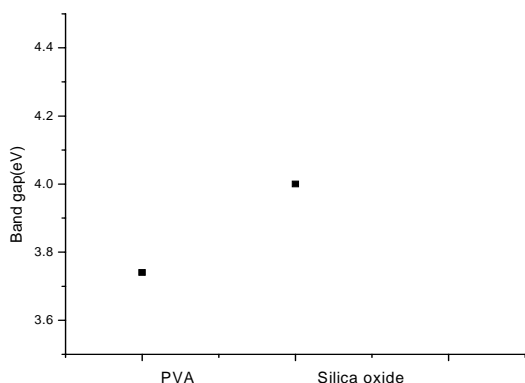


Fig 5. Band gap of ZnS:Mn with PVA and silica oxide.

It is found that the band gap energy of the resulting nanoparticles shows marked increment as compared with that of ZnS bulk materials (3.70 eV). The shift of the absorption spectra is attributed to the quantum confinement of charge carriers in the nanoparticles.

Fig. 5 clearly shows bandgap variation in ZnS capped with polymers (PVA and Silica oxide).

Interestingly TEM studies reveals the individual crystallite sizes ~ 10 nm {Fig.4 (a)} and ~ 20 nm {Fig.4(b)} for silica oxide and PVA coated ZnS respectively which is consistent with the theoretical calculations from XRD data and model based calculations from SAXS.

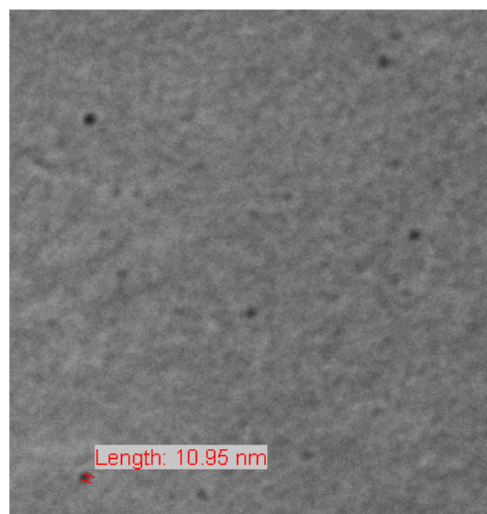


Fig. 4.(a) TEM image of Silica oxide coated Mn doped ZnS.

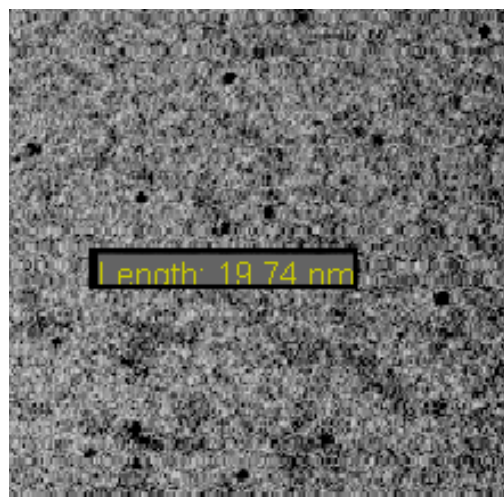


Fig.4. (b) TEM image of PVA coated Mn doped ZnS.

4. Conclusions

In the present paper, we report the wet chemical synthesis of the ZnS: Mn nanoparticles capped with

organic and inorganic capping agents (silica oxide and narrow PVA). The nanoparticles show better particle size stability and grain size distribution in ZnS:Mn capped with silica oxide. We also observed an increase in size dependent Stokes shift of the PL maximum relative to the absorption onset as the particle size decreases. Furthermore, band gap enlargement is also in agreement with the theoretical calculation based on the effective mass model. The band gap of nanoparticles can be tailored with different capping agents as capping agent restricts the particle growth. Optimum conditions and mechanisms required to synthesize capped nanoparticles of Mn-doped ZnS were explored. Efforts are currently underway to cap the ZnS nanoparticles with other agents to restrict particle growth.

Acknowledgement

We would like to acknowledge the support of NAC members and R.N.Bhargava for guidance.

References

- [1] H. Cnilk., J. Liang, S. G. Cloutier, N. Koukin, I. M. Xu, *Appl. Phys. Lett.* **84**, 3376(2004)
- [2] H. Ohta, K. Kawamura, M. Orita, N. Hirano, N. Sarkura, H. Hosono, *Appl. Phys. Lett.* **77**, 47(2000)
- [3] M. H. Huang, S. Mao, H. Feric, H. Feric, H. Yan, Y. Wu, H. Kind, E. Weber, R. Russo, P. Yang, *Science* **292**, 1897 (2001)
- [4] R. Rossetti, J. L. Ellison, J. M. Gibson, L. E. Brus, *J. Chem. Phys.* **80**, 4464 (1984).
- [5] Y. Wang, W. Mahler, *Opt. Commun.* **61**, 233 (1987).
- [6] R. N. Bhargava, D. Gallagher, *Phys. Rev. Lett.* **72**, 416 (1994).
- [7] C. B. Murray, D. J. Norris, and M. G. Bawendi, *J. Am. Chem. Soc.* **115**, 8706 (1993).
- [8] A. A. Khosravi, M. Kundu, B. A. Kuruvilla, G. S. Shekhawat, *Appl. Phys. Lett.* **67**, 2506 (1995).
- [9] R. Rossetti, R. Hull, J. M. Gibson, L. E. Brus, *J. Chem. Phys.* **82**, 552 (1985).
- [10] T. Igarashi, T. Isobe, M. Senna, *Phys. Rev. B* **56**, 6444 (1995).
- [11] H. Tang, G. Y. Xu, L. Q. Weng, L. J. Pan, L. Wang, *Acta Mater.* **52**, 1489 (2004)
- [12] Y. Wang, N. Herron, *J. Phys. Chem.* **95**, 525 (1991).
- [13] M. Huang, S. Mao, H. Feit, N. Tran, E. Weber, P. Yang, *Adv. Matter.* **13**, 113 (2001).
- [14] T. Y. Kim, J. Y. Kim, M. S. Kumar, E. K. Suh, K. S. Nahm, *J. Cryst. Growth* **270**, 491 (2004).
- [15] L. Spanhel, M. A. Anderson, *J. Am. Chem. Soc.* **113**, 2826 (1991).
- [16] J. Dutta, H. Hofmann, *Encyclopedia of Nanoscience and Nanotechnology* **9**, 617 (2004).
- [17] B. D. Gates, Q. Xu, J. C. Love, D. B. Wolfe, G. M. Whitesides, *Annu-Rev. Mater. Res.* **34**, 339 (2004).
- [18] T. A. Kennedy, E. R. Giaser, P. B. Klein, R. N. Bhargava, *Phys. Rev. B* **52**, R14356 (1995).
- [19] D. Gallagher, W. E. Heady, J. M. Racz, R. N. Bhargava, *J. Mater. Res.* **10**, 870 (1995).
- [20] T. A. Kennedy, E. R. Glaster, P. B. Klein, R. N. Bhargava, *Phys. Rev. B* **52**, R14356 (1995).
- [21] H. Ito, T. Tanaka, F. Minami, H. Akinaga, *J. Lumin.* **72-74**, 342 (1997).
- [22] L. E. Brus, *J. Chem. Phys.* **80**, 4403 (1984).
- [23] M. S. Hyberstsen, *Phys. Rev. Lett.* **72**, 1514 (1994).
- [24] H. Fu, A. Zunger, *Phys. Rev. B* **56**, 1496 (1997).
- [25] E. F. Kaelble, *Handbook of X-rays*, Mc Graw-Hill, New York, 1967.

*Corresponding author: prinsa.verma@gmail.com